JTTEE5 5:303-309

Energy Absorption Capacity of Thermally Sprayed Aluminum Friction Dampers

S. Ono, K. Nakahira, S.Tsujioka, and N. Uno

When buildings are subjected to earthquakes, dampers are effective in decreasing their failure by absorbing the input energy. An objective of this study is to develop a new type of friction damper, on whose faying surface aluminum is sprayed, and the double friction joint is tightened with a high-strength bolt. When slip occurs on this friction damper, the slip coefficient is high and comparatively stable. Specimens of the friction damper were tested under static and dynamic cyclic loading conditions to investigate the effect of the condition of the faying surface on the hysteresis characteristics. The parameters of the test are thickness of sprayed aluminum, initial clamping force (contact pressure), loading program, type of sprayed metal, and sprayed side of the plate. Results indicate that relationships exist between the thickness of sprayed aluminum and the clamping force to obtain stable slip load.

Keywords aluminum sprayed coating, friction damper, initial clamping force (contact pressure), static and dynamic hysteresis characteristics, thickness of sprayed aluminum

1. Introduction

FAILURE or collapse of a building can be caused under the excessive force of an earthquake or wind load. Friction dampers are effective in decreasing the failure of buildings by absorbing the input energy (Ref 1-18). An example of a frame equipped with a friction damper is illustrated in Fig. 1. The results of the analysis of elastoplastic response of the single degree-of-freedom shear model shown in Fig. 1 are shown in Fig. 2. It is confirmed that friction dampers are effective in decreasing the failure of frames (Ref 19).

However, it is very important to adjust the level of friction force. Because residual deformation might exist on the building after an earthquake, even if failure or collapse did not occur, it should be possible to inspect and replace the dampers (Ref 1).

The object of this study is to develop a new type of friction damper with a double friction joint that is tightened with high-strength bolts as shown in Fig. 3. Aluminum is sprayed on the faying surface of this friction damper. When slip occurs on this friction damper, the coefficient of slip shows a high value of approximately 0.8 to 1.0 and the hysteresis characteristic of this friction damper is comparatively stable (Ref 20). Applying this behavior, it is possible to form a high-strength, compact, and lightweight friction damper. One characteristic of this friction damper is that the slip load can be adjusted by changing the initial clamping force and the number of bolts.

The main aim of this research was to investigate the effect of the condition of the faying surface on the hysteresis characteristics. The experimental study was designed to observe the coefficient of slip and the range of the stable hysteresis characteristic (in the following text, the term is simply "the stable range") under static and dynamic cyclic loads.

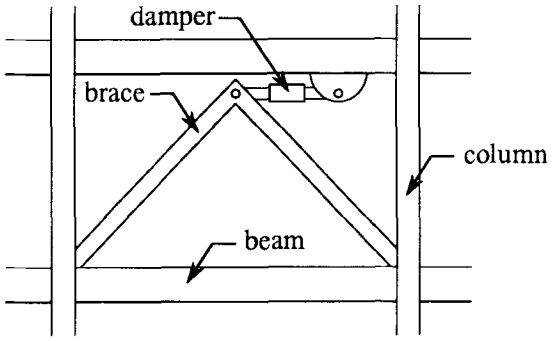

Fig. 1 Example of a frame equipped with a friction damper

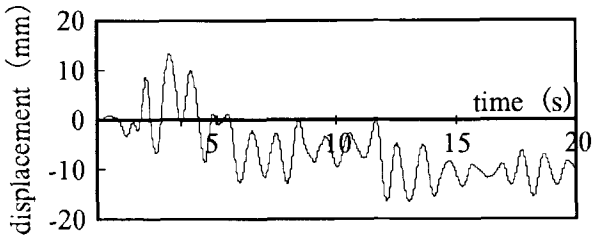

(a) only the frame (not equipped with a friction damper)

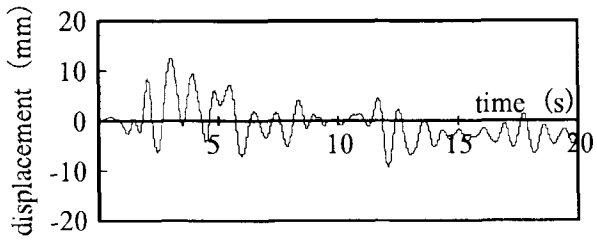

(b) the frame equipped with a friction damper

Fig. 2 Time histories of displacement of the frame

S. Ono, Department of Architectural Engineering, Faculty of Engineering, Osaka University, 2-1, Yamadaoka, Suita, Osaka, 565, Japan; **K. Nakahira,** Planners, Architects, Engineering & Contractors, Building Design Department, Takenaka Corporation, 2-3-10, Nishi Honmachi, Nishi-ku, Osaka, 550, Japan; **S. Tsujioka,** Department of Architectural Engineering, Faculty of Engineering, Fukui Institute of Technology, 3-6-1, Gakuen, Fukui, 910, Japan; and **N. Uno,** Technical Development Center, Nippon Steel Corporation, 20-1, Shintomi, Futtsu, Chiba, 299-12, Japan.

2. Static Cyclic Loading Test

2.1 *Experimental Procedure*

Each of the specimens tested under the static cyclic load is composed of the double friction joint tightened with a high-strength bolt (F10T M20), as shown in Fig. 3. The sides of the outer plates are chamfered before spraying with aluminum, and the inner plate has a slot hole. Both surfaces of this inner plate are polished to mirror finish (less than R_{max} = 1.5 μm) to avoid damage from the sprayed aluminum by scratching. To study the effect of the surface roughness of mirror-finished plates, the inner plate of No. 9 and 10 are flat finished(less than R_{max} = 12 μm). Plate washers with 25 mm thickness were used in order to have a uniform contact pressure.

The list of 16 specimens is shown in Table 1. Parameters are thickness of sprayed aluminum, initial clamping force (contact pressure), and loading program. The loading programs are increasing- and decreasing-repeated load, as shown in Fig. 4. Each force displacement of ±5, ±10, and ±20 mm is repeated three times.

2.2 *Results and Discussions*

The P-δ relations of typical specimens obtained from the experiment are shown in Fig. 5, where P represents the loads applied to the specimen and δ represents the relative displacement between inner plate and outer plate (see Fig. 3). The B-δ relations of typical specimens are shown in Fig. 6, where B represents the axial force of the bolt. Results of the static cyclic

Table 1 List of specimens in static cyclic loading test

Specimen No.	Specimen code(a)	Surface finish of inner plate	Thickness of sprayed aluminum, μm			Contact pressure, MPa	Loading program
			Aim value	Measured value (Average)			
1	MA50I-15	Mirror finish (R_{max} = 1.5 μm)	40-60	54	64	25.7	Increasing
2	MA50I-15	Mirror finish (R_{max} = 1.5 μm)	40-60	62	52	25.7	Decreasing
3	MA50I-15	Mirror finish (R_{max} = 1.5 μm)	90-110	114	125	25.7	Increasing
4	MA50I-15	Mirror finish (R_{max} = 1.5 μm)	90-110	115	101	25.7	Decreasing
5	MA50I-15	Mirror finish (R_{max} = 1.5 μm)	140-160	145	150	17.2	Increasing
6	MA50I-15	Mirror finish (R_{max} = 1.5 μm)	140-160	158	165	17.2	Decreasing
7	MA50I-15	Mirror finish (R_{max} = 1.5 μm)	140-160	153	150	25.7	Increasing
8	MA150D-15	Mirror finish (R_{max} = 1.5 μm)	140-160	140	138	25.7	Decreasing
9	FA150I-15	Flat finish (R_{max} = 12 μm)	140-160	168	148	25.7	Increasing
10	FA150D-15	Flat finish (R_{max} = 12 μm)	140-160	150	165	25.7	Decreasing
11	MA400I-15	Mirror finish (R_{max} = 1.5 μm)	390-410	463	420	25.7	Increasing
12	MA400I-15	Mirror finish (R_{max} = 1.5 μm)	390-410	430	410	25.7	Decreasing
13	MA400I-15	Mirror finish (R_{max} = 1.5 μm)	590-610	663	600	17.2	Increasing
14	MA400I-15	Mirror finish (R_{max} = 1.5 μm)	590-610	590	675	17.2	Decreasing
15	MA400I-15	Mirror finish (R_{max} = 1.5 μm)	590-610	615	710	25.7	Increasing
16	MA600D-15	Mirror finish (R_{max} = 1.5 μm)	590-610	600	620	25.7	Decreasing

(a) The specimen code of generic form "XY123Z-45" refers to "X" = M: mirror finish or F: flat finish; "Y" = A: aluminum; "123" = thickness (in μm) of sprayed aluminum; "Z" = I: the increasing load or D: the decreasing load; and "45" = initial clamping force (×10 kN)

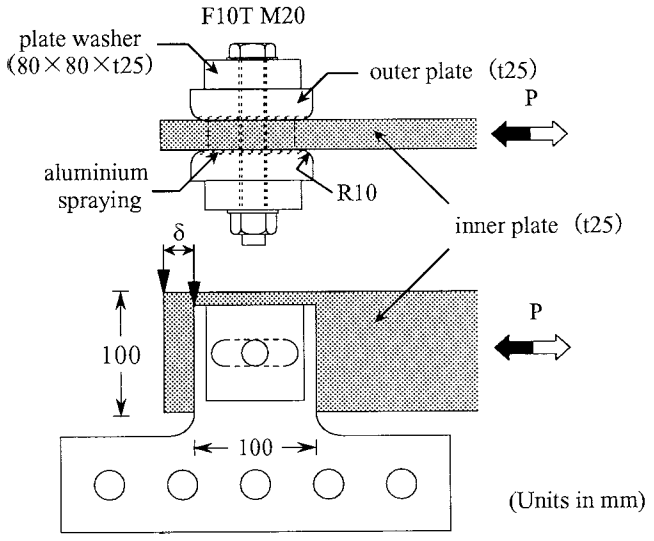

Fig. 3 Test specimen for the static cyclic loading test

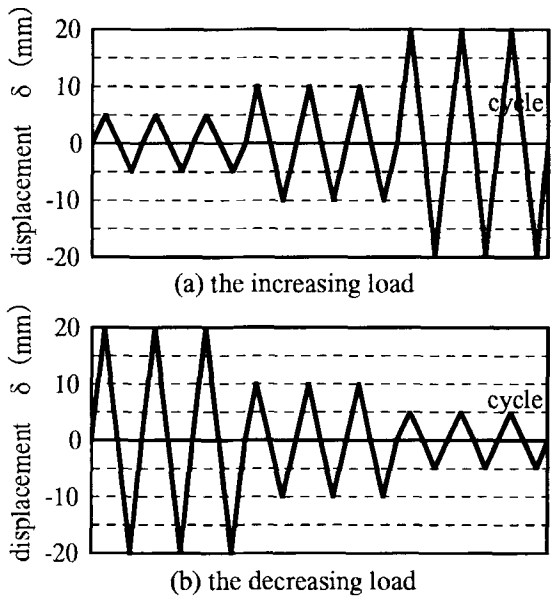

Fig. 4 Loading program

loading test are summarized in Table 2, in which the average of the slip load is the area surrounded by each hysteresis loop divided by each corresponding displacement.

When the coating thickness is about 50 to 150 μm (No. 1 through 8), the slip load is nearly equal under both the increasing- and decreasing-loads, and the coefficient of variation (standard deviation divided by the mean) of the slip load and the axial force of the bolt area small. The coefficient of slip of 100 to 150 μm specimen has a comparatively stable value of about 0.9. The coefficient of slip is approximately 0.65 in the specimens with a 50 μm thick coating, which is low compared with other specimens. In the specimens with 150 μm aluminum, when the initial clamping force increases by a factor 1.5, the slip load increases by 1.25, and the coefficient of slip decreases by 10%. Under the increasing load, the specimens with a flat-finished inner plate show the same hysteresis characteristics as the mirror-finished specimen. However, under the decreasing load (No. 10), the slip load decreases by 10 to 20%.

The specimens with more than 400 μm aluminum, when tested under a decreasing load (in No. 11 through 16), exhibit slip loads of almost the same value as those in other specimens, but the coefficient of slip shows a value of more than 1.0. The slip load in the specimens of the decreasing load decreases on further cycling. The coefficient of variation of both the slip load and the axial force of the bolt are large. In the specimens of the decreasing load, the coefficient of slip shows a low value compared with the specimen of the increasing load. There are no differences in coefficient of slip between the positive and negative half-cycle load in all the specimens.

As a result, the most suitable thickness of sprayed aluminum is about 50 to 150 μm.

3. Dynamic Cyclic Loading Test

3.1 *Experimental Procedure*

Specimens used in the dynamic cyclic loading test are shown in Fig. 7. This shape is almost the same as the case of the static cyclic loading test. Parameters studied were the type of sprayed metal, the sprayed side of the plate(s), thickness of sprayed metal, and initial clamping force (contact

Table 2 Results of static cyclic loading test

Specimen No.	Specimen code(a)	Initial clamping force, kN	Axial force of the bolt		Coefficient of slip		Slip load				Ratio (positive/ negative)
							Positive half-cycle load		Negative half-cycle load		
			Average, kN	Coefficient of variation	Positive half-cycle load	Negative half-cycle load	Average, kN	Coefficient of variation	Average, kN	Coefficient of variation	
1	MA50I-15	147	147	0.015	0.63	0.65	185	0.085	195	0.072	0.95
2	MA50D-15	149	138	0.056	0.66	0.65	171	0.061	174	0.074	0.98
3	MA100I-15	147	148	0.043	0.90	0.93	261	0.087	267	0.079	0.97
4	MA100D-15	146	136	0.047	0.82	0.86	220	0.061	230	0.069	0.95
5	MA150I-10	98	101	...	0.96	1.09	185	0.072	217	0.048	0.85
6	MA150D-10	99	99	0.066	0.93	0 96	186	0.019	190	0.043	0.98
7	MA150I-15	146	148	0.040	0.85	0.89	247	0.060	255	0.061	0.97
8	MA150D-15	145	144	0.045	0.79	0.83	230	0.021	242	0.055	0.95
9	FA150I-15	145	143	0.040	0.91	0.91	264	0.058	263	0.052	1.00
10	FA150D-15	165	153	0.040	0.92	0.82	272	0.059	269	0.038	1.01
11	MA400I-15	143	130	0.126	1.03	1.03	254	0.197	252	0.173	1.01
12	MA400D-15	143	122	0.186	0.71	0.77	153	0.354	161	0.387	0.95
13	MA600I-10	99	91	0.093	1.36	1.36	235	0.163	232	0.136	1.01
14	MA600D-10	103	73	0.418	...	...	120	0.408	126	0.344	0.96
15	MA600I-15	145	137	0.082	1.12	1.11	271	0.190	274	0.148	0.99
16	MA600D-15	147	117	0.218	0.93	0.87	176	0.436	170	0.401	1.03

(a) Code details are presented in Table 1.

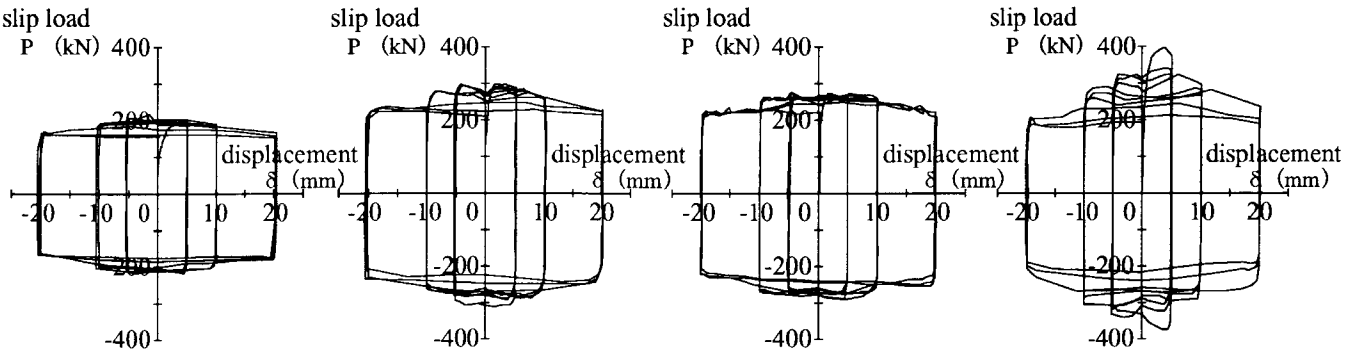

(a) No. 1 <MA50I-15> (b) No. 3 <MA100I-15> (c) No. 7 <MA150I-15> (d) No. 11 <MA400I-15>

Fig. 5 *P*-δ (load-displacement) relations in static cyclic loading

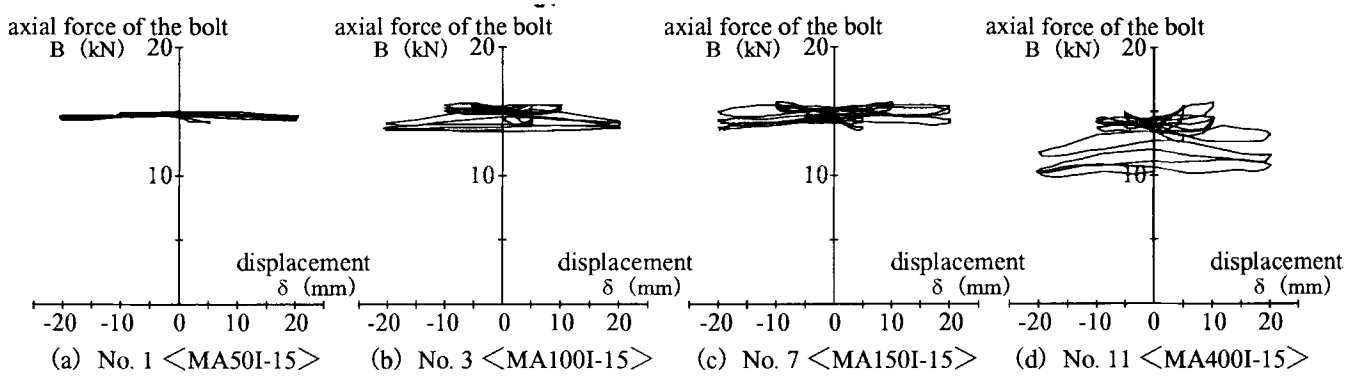

Fig. 6 B-δ (axial force of the bolt-displacement) relations in static cyclic loading test

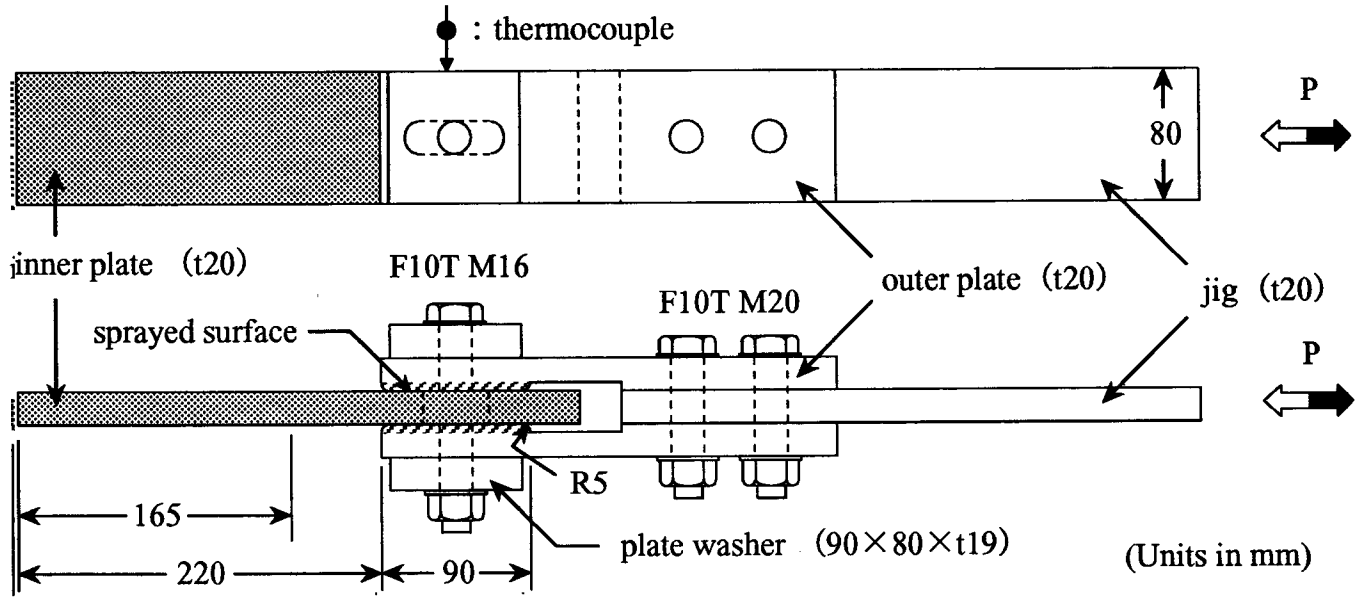

Fig. 7 Test specimen for the dynamic cyclic loading test

Table 3 List of specimens in the dynamic cyclic loading test

Specimen No.	Specimen code(a)	Conditions of faying surface: Kind of sprayed metal	Sprayed side of the plate	Thickness of sprayed metal, μm: Aim value	Measured value	(Average)	Contact pressure, MPa
1	DA0505O	Aluminum	Outer plate	40-60	70	70	8.9
2	DA0510O	Aluminum	Outer plate	40-60	80	80	17.8
3	DA1005O	Aluminum	Outer plate	90-110	120	120	8.9
4	DA1010O	Aluminum	Outer plate	90-110	120	123	17.8
5	DA1510O	Aluminum	Outer plate	140-160	180	180	17.8
6	DA1510I	Aluminum	Inner plate	140-160	148	148	17.8
7	DC1510I	Copper	Inner plate	140-160	153	151	8.9
8	DP1005O	Lead-tin	Outer plate	90-110	120	123	17.8

(a) Follow prior example in Table 1

pressure), as shown in Table 3. The thickness of sprayed metal varied between 50 to 150 μm on consideration of static repeated loading tests. Both sides of inner plate were sprayed in two specimens (No. 6 and 7), while in other specimens the outer plates have the sprayed surface. The thickness was accurately produced by polishing the surface after spraying.

Each specimen was subjected to a sinusoidal wave of displacement amplitude ±15 mm at 1 Hz, by using a servocontrolled fatigue testing machine. The axial force of the bolt was measured by strain gages, placed on the head of the bolt, and the temperature of the specimen was measured by a thermocouple set at the edge of the inner plate during loading (see Fig. 7).

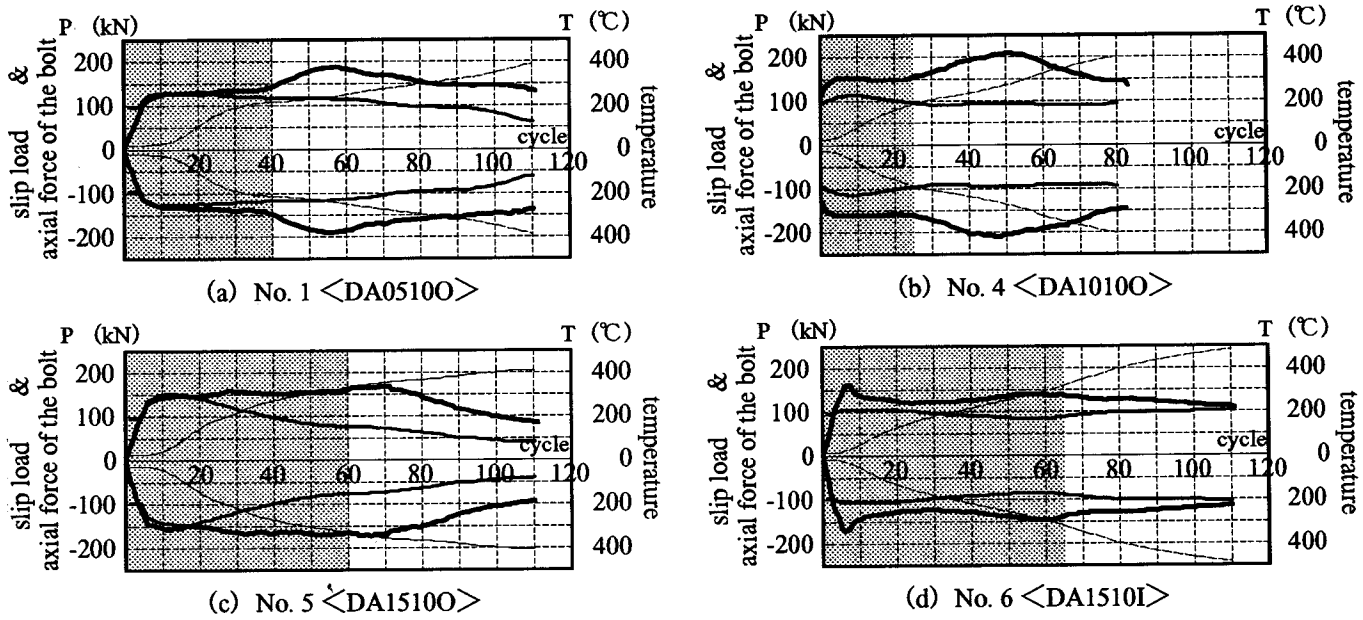

Fig. 8 *P*, *B*, and *T* (slip load, axial force of the bolt, and temperature) in each cycle. — *P*, average slip load; —*B*, average axial force of the bol t; - -*T*, average temperature

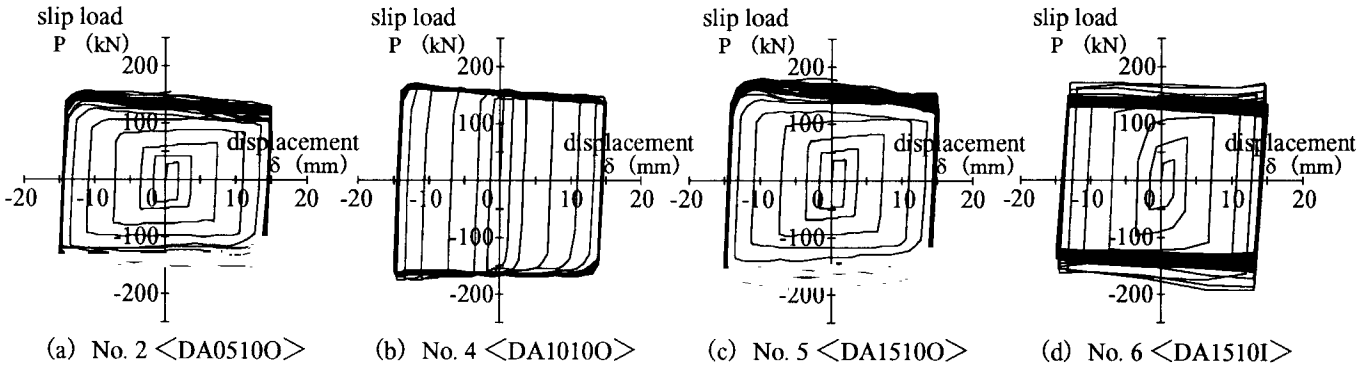

Fig. 9 *P*-δ relations in the stable range (the dynamic cyclic loading test)

3.2 *Results and Discussions*

Figure 8 shows the average slip load *P*, the average axial force of the bolt *B*, and the average temperature *T* plotted in each cycle. The shaded area in Fig. 8 shows the stable range for each specimen. Results calculated in the stable range are summarized in Table 4. The *P*-δ relations are shown in Fig. 9 for the same range. While loading specimen No. 4, near the 37th cycle the slip load exceeded the value expected and the testing was stopped. This specimen was reloaded after resetting.

In the specimens with aluminum spraying of 50 μm thickness, when the initial clamping force increases by a factor of 2.0, the slip load increases by a factor of 0.6 and the slip load increases by 1.6 in the stable range (see Fig. 8). The total area surrounded by each hysteresis loop in specimen No. 1 and 2 is nearly equal. The stable range is not related to initial clamping force for specimens with aluminum of 100 μm thickness. When the initial clamping force increases by a factor of 2.0, the slip load increases by 1.5. In the case of aluminum of 50 to 100 μm thickness, when the initial clamping force increases by a factor of 2.0, the slip load decreases by about 10 to 20%. In aluminum spraying of 150 μm thickness, the stable range and the coefficient of slip show the same value, irrespective of the sprayed side of the plate(s). Compared with the specimens sprayed on outer plates, the slip load of the specimens sprayed on the inner plate is lower in the stable range. The rise of temperature of the specimens sprayed on the inner plate is larger than that of the specimens sprayed on outer plates after the stable range.

The copper-sprayed specimen exhibits a stable range in only the first 20 cycles. Compared with the specimens with aluminum contents, the slip load in the stable range is nearly equal, but the coefficient of slip is about 90%. In the specimen of sprayed lead-tin alloy, the hysteresis characteristic is stable through whole cycles, as is the axial force of the bolt. However, compared with the specimens of aluminum or copper spraying, the slip load and the coefficient of slip shows a very low value.

As shown in the *P*-δ relations in Fig. 9, the slip load of the specimens of aluminum or copper coatings (except No. 4) increases with increasing displacement at early cycles. Such behavior was not observed in the hysteresis loops tested under the

Table 4 Results of the dynamic cyclic loading test

Spec. No.	Spec. code(a)	Number of cycle	Cum. slip, mm	Initial clamping force, kN	Axial force of the bolt		Coefficient of slip		Slip load				Ratio (pos./ neg.)	Temp. (max), °C
									Positive half-cycle load		Negative half-cycle load			
					Avg., kN	Coefficient of variation	Pos. half-cycle load	Neg. half-cycle load	Avg., kN	Coefficient of variation	Avg., kN	Coefficient of variation		
1	DA0505O	70	4040	49	63	0.090	0.62	0.66	78	0.076	75	0.067	1.04	223
2	DA0510O	40	2239	98	119	0.072	0.54	0.57	130	0.044	127	0.041	1.02	221
3	DA1005O	32	1761	50	76	0.178	0.63	0.68	95	0.167	90	0.147	1.06	197
4	DA1010O	25	1339	97	117	0.061	0.71	0.76	158	0.006	151	0.012	1.05	185
5	DA1510O	60	3441	98	132	0.222	0.69	0.73	152	0.046	148	0.028	1.03	335
6	DA1510I	65	3701	97	105	0.083	0.68	0.70	141	0.076	135	0.064	1.04	324
7	DC1510I	20	1028	97	109	0.057	0.61	0.64	136	0.036	132	0.035	1.03	147
8	DP1005O	111	6440	49	58	0.022	0.22	0.23	16	0.135	14	0.149	1.14	73

(a) Make the same adjustment as in prior Table 1.

static cyclic load (see Fig. 5). The reason for this behavior is not clear. However, the reloaded specimen (No. 4) shows a stable slip load from early cycles. Therefore, 5 or 6 cycles is effective to obtain a stable hysteresis characteristic from early cycles if necessary.

There are no differences of coefficient of slip between positive and negative halves of the load cycle in all the specimens. When a severe earthquake occurs, the amount of cumulative slip of the damper is required to be about 60 cm (Ref 19). The amount of cumulative slip of the damper observed in this experimental study sufficiently exceeds this value.

The results of the examination indicate that the suitable sprayed side of the plate(s) is the outer plate, the adequate kind of sprayed metal is aluminum, and in the case of aluminum spraying of about 50 to 150 μm thickness, the amount of cumulative slip of this friction damper is sufficient compared with analytical value.

4. Conclusions

This study indicates that suitable characteristics of metal sprayed friction damper are as follows:

- Sprayed side of the plate(s): outer plates
- Type of sprayed metal: aluminum
- Thickness of sprayed metal: thickness of the order of 50 to 150 μm

The following results are from tests performed under the above conditions:

- In the case of 50 μm thick aluminum, the amount of cumulative slip depends on the initial clamping force.
- In the case of 100 μm thick aluminum, the amount of cumulative slip is independent of the initial clamping force.
- The amount of cumulative slip in the stable range sufficiently satisfies the amount of cumulative slip in the case of a severe earthquake.
- As a result of the static cyclic loading test, this friction damper can be applied to an earthquake of large initial amplitude since the results (slip load, etc.) show no difference between the increasing and the decreasing load.
- Five or six cycles are effective to obtain a stable hysteresis characteristic.
- Compared with dynamic cyclic loading tests, the coefficient of slip of a static cyclic loading test is 20 to 30% larger.

Acknowledgments

The authors would like to acknowledge the continuing guidance and many helpful suggestions of Dr. K. Inoue, Associate Professor of Osaka University. The authors wish to express their gratitude to Dr. T. Segawa and Dr. T. Tanaka of Takenaka Corporation, Dr. Y. Harada and Mr. M. Okitsu of Tocalo Corporation, for many helpful suggestions and observations. The authors wish to thank Mr. J. Tokuyama of Obayashi Corporation, a former graduate student of Osaka University, Ms. A. Shimizu of Konoike Construction Co., Ltd., a former student of Osaka University, and the members of Tsujioka Laboratory of Fukui Institute of Technology, for their assistance in the experiment of this paper.

References

1. "Recommendation for the Design of Base Isolated Buildings," Architectural Institute of Japan, 1989 (in Japanese)
2. T. Teramoto, H. Kitamura, I. Hashinaka, K. Araki, and K. Takada, Application of Friction Damper to Highrise Steel Building (Part 1), *Summaries of Technical Papers of Annual Meeting Architectural Institute of Japan, Structure I-B,* 1987, p 873-878 (in Japanese)
3. T. Teramoto, M. Keii, S. Sakamoto, K. Takada, and K. Araki, Application of Friction Damper to Highrise Steel Building (Part 2), *Summaries of Technical Papers of Annual Meeting Architectural Institute of Japan, Structure I-B,* 1987, p 873-878 (in Japanese)
4. T. Teramoto, M. Keii, and H. Kitamura, Application of Friction Damper to Highrise Steel Building (Part 3), *Summaries of Technical Papers of Annual Meeting Architectural Institute of Japan, Structure I-B,* 1987, p 873-878 (in Japanese)
5. N. Katayama, T. Teramoto, H. Kihara, T. Kobori, N. Iida, and K. Takada, Application of Friction Damper to Highrise Steel Building (Part 4), *Summaries of Technical Papers of Annual Meeting Architectural Institute of Japan, Structure I-B,* 1989, p 665-668 (in Japanese)
6. T. Kobori, T. Teramoto, and H. Kihara, Application of Friction Damper to Highrise Steel Building (Part 5), *Summaries of Techni-*

cal Papers of Annual Meeting Architectural Institute of Japan, StructureI-B, 1989, p 665-668 (in Japanese)

7. M. Kimura, Y. Higashihata, K. Inoue, N. Nakayama, K. Takahashi, and Y. Nanami, The Experimental Study on Friction Damper with H.T.B. (Part 1), *Summaries of Technical Papers of Annual Meeting Architectural Institute of Japan, Structure I-B,* 1992, p 1051-1052 (in Japanese)
8. M. Kimura, N. Nakayama, K. Inoue, A. Aizawa, Y. Higashihata, S. Minewaki, and Y. Nanami, The Experimental Study on Friction Damper with H.T.B. (Part 2), *Summaries of Technical Papers of Annual Meeting Architectural Institute of Japan, Structure I-B,* 1993, p 1051-1052 (in Japanese)
9. N. Nakayama, Y. Higashihata, A. Aizawa, K. Inoue, S. Minewaki, and K. Yofune, The Experimental Study on Friction Damper with H.T.B. (Part 3), *Summaries of Technical Papers of Annual Meeting Architectural Institute of Japan, Structure I-B,* 1993, p 577-580 (in Japanese)
10. N. Nakayama, K. Inoue, A. Aizawa, S. Minewaki, and K. Toyama, The Experimental Study on Friction Damper with H.T.B. (Part 4), *Summaries of Technical Papers of Annual Meeting Architectural Institute of Japan, Structure I-B,* 1994, p 1037-1038 (in Japanese)
11. S. Hayama, K. Nagai, T. Uno, H. Takai, T. Koide, and T. Nishiide, Study on the Feasibility of a Base Isolation System (Part 1), *Summaries of Technical Papers of Annual Meeting Architectural Institute of Japan, Structure I-B,* 1987, p 841-848 (in Japanese)
12. T. Uno, K. Nagai, T. Koide, and T. Nishiide, Study on the Feasibility of a Base Isolation System (Part 2), *Summaries of Technical Papers of Annual Meeting Architectural Institute of Japan, Structure I-B,* 1987, p 841-848 (in Japanese)
13. H. Takai, K. Nagai, T. Koide, and T. Nishiide, Study on the Feasibility of a Base Isolation System (Part 3), *Summaries of Technical Papers of Annual Meeting Architectural Institute of Japan, Structure I-B,* 1987, p 841-848 (in Japanese)
14. T. Koide, K. Nagai, T. Uno, and H. Takai, Study on the Feasibility of a Base Isolation System (Part 4), *Summaries of Technical Papers of Annual Meeting Architectural Institute of Japan, Structure I-B,* 1987, p 841-848 (in Japanese)
15. T. Uno, K. Nagai, and Y. Ito, Study on the Feasibility of a Base Isolation System (Part 5), *Summaries of Technical Papers of Annual Meeting Architectural Institute of Japan, Structure I-B,* 1988, p 435-441 (in Japanese)
16. H. Takai, T. Uno, and K. Asano, Study on the Feasibility of a Base Isolation System (Part 6), *Summaries of Technical Papers of Annual Meeting Architectural Institute of Japan, Structure I-B,* 1988, p 435-441 (in Japanese)
17. K. Asano, Y. Ito, and T. Yamasaki, Study on the Feasibility of a Base Isolation System (Part 7), *Summaries of Technical Papers of Annual Meeting Architectural Institute of Japan, Structure I-B,* 1988, p 435-441 (in Japanese)
18. Y. Ito, M. Ichikawa, K. Nagai, and T. Tomii, Study on the Feasibility of a Base Isolation System (Part 8), *Summaries of Technical Papers of Annual Meeting Architectural Institute of Japan, Structure I-B,* 1988, p 435-441 (in Japanese)
19. K. Inoue, J. Tokuyama, A. Shimizu, and S. Ono, Seismic Responses of Shear-Type Multi-Story Model Equipped with the Friction Damper (Part 1, 2), *Summaries of Technical Papers of Annual Meeting Architectural Institute of Japan, Structure I-B,* 1994, p 649-652 (in Japanese)
20. K. Inoue, S. Ono, and J. Tokuyama, Study on Feasibility of a Base Isolation System (Part 1, 2), *Summaries of Technical Papers of Annual Meeting Architectural Institute of Japan, Structure I-B,* 1993, p 587-590 (in Japanese)
21. *Thermal Spraying Handbook,* Japan Thermal Spraying Society, 1991 (in Japanese)
22. *JIS Handbook: Non-Ferrous Metals & Metallurgy,* Japan Standards Association, 1993 (in Japanese)
23. *JIS Handbook: Metal Surface Treatment,* Japan Standards Association, 1993 (in Japanese)
24. S. Ono, K. Nakahira, S. Tsujioka, T. Segawa, and T. Tnaka, Static and Dynamic Hysteresis Characteristic of the Aluminium Spraying Friction Damper (Part 1, 2), *Summaries of Technical Papers of Annual Meeting Architectural Institute of Japan, Structure I-B,* 1994, p 757-760 (in Japanese)
25. S. Ono, K. Nakahira, S. Tsujioka, and I. Inoue, Static and Dynamic Hysteresis Characteristic of the Aluminium Spraying Friction Damper (Part 1, 2), *J. Struct. Eng.,* Vol 41B, 1995, p 1-8 (in Japanese)
26. S. Ono, K. Nakahira, S. Tsujioka, and N. Uno, Energy Absorption Capacity of Thermally Sprayed Aluminium Friction Damper, *Proc. 14th Int. Thermal Spray Conference,* 1995, p 169-174